Stop Blaming Hopping Conduction in Nanocrystal Arrays, Use it for Active Photonics!

Nicolas Ledos, Tung H Dang, Mariarosa Cavallo, Huichen Zhang, Erwan Bossavit, Adrien Khalili, Lam Nguyen Do, Charlie Gréboval, Sandrine Ithurria, James K Utterback, et al.

ADVANCED MATERIALS TECHNOLOGIES
www.advmattechnol.de

Stop Blaming Hopping Conduction in Nanocrystal Arrays, Use it for Active Photonics!

*Nicolas Ledos, Tung H. Dang, Mariarosa Cavallo, Huichen Zhang, Erwan Bossavit, Adrien Khalili, Lam Nguyen Do, Charlie Gréboval, Sandrine Ithurria, James K. Utterback, Debora Pierucci, Gregory Vincent, Angela Vasanelli, and Emmanuel Lhuillier**

Nanocrystals (NCs) are now established building blocks for photonic applications. However, their integration for optoelectronics has not yet reached the same level of maturity, in part due to the perceived bottleneck that is the inherent limited mobility resulting from hopping conduction. Significant efforts are made to improve this mobility, notably by tuning the particle surface chemistry to enable larger interparticle electronic coupling, and values of mobility of ≈10 $cm^2 V^{-1} s^{-1}$ have been achieved. It is acknowledged that this value remains significantly lower than those obtained in 2D electron gases but is on par with the mobility reported for vertical transport in epitaxially grown heterostructures with similar confinement energies. Since there appears to be limited perspectives for further increasing mobility values, a suggestion is made that efforts should instead be directed toward exploring the potential benefits offered by hopping conduction. One of these benefits is the bias dependence of the diffusion length, which plays a key role in designing bias-reconfigurable optical responses for NC-based devices. Some recent achievements in building bias-activated devices will be reviewed and the essential criteria for designing future structures will be discussed. Ultimately, hopping conduction is an opportunity to generate new functionalities that low-disorder materials would be unable to provide.

1. A Brief History of Charge Carrier Transport in Nanocrystal Thin Films

Initially, the interest for semiconductor NCs lay mainly in their optical properties. As low-dimensional semiconductors, they offer the advantage of a tunable optical spectrum based simply on size. Indeed, introducing quantum confinement to semiconductors by reducing their dimensionality provides a means to continuously tune the bandgap values, as illustrated in **Figure** 1a, which emerged as an alternative to alloying. This phenomenon not only increases the band edge energy compared to bulk materials but also discretizes their density of states, which provides additional properties to nanocrystals compared to bulk and thin films. Thanks to these properties, nanocrystals have achieved remarkable success in various applications as optically active

N. Ledos, T. H. Dang, M. Cavallo, H. Zhang, E. Bossavit, A. Khalili, L. N. Do, C. Gréboval, J. K. Utterback, D. Pierucci, E. Lhuillier
Sorbonne Université
CNRS
Institut des NanoSciences de Paris (INSP)
4 place jussieu, Paris 75005, France
E-mail: el@insp.upmc.fr

T. H. Dang, A. Vasanelli
Laboratoire de physique de l'Ecole Normale Supérieure
ENS
Université PSL
CNRS
Sorbonne Université
Université Paris Cité
Paris 75005, France

E. Bossavit
Synchrotron SOLEIL
L'Orme des Merisiers
Départementale 128, Saint-Aubin 91190, France

S. Ithurria
Laboratoire de Physique et d'Etude des Matériaux
ESPCI-Paris
PSL Research University
Sorbonne Université
CNRS UMR 8213
10 rue Vauquelin, Paris 75005, France

G. Vincent
DOTA
ONERA
Université Paris Saclay
Palaiseau 91123, France

DOI: 10.1002/admt.202301463

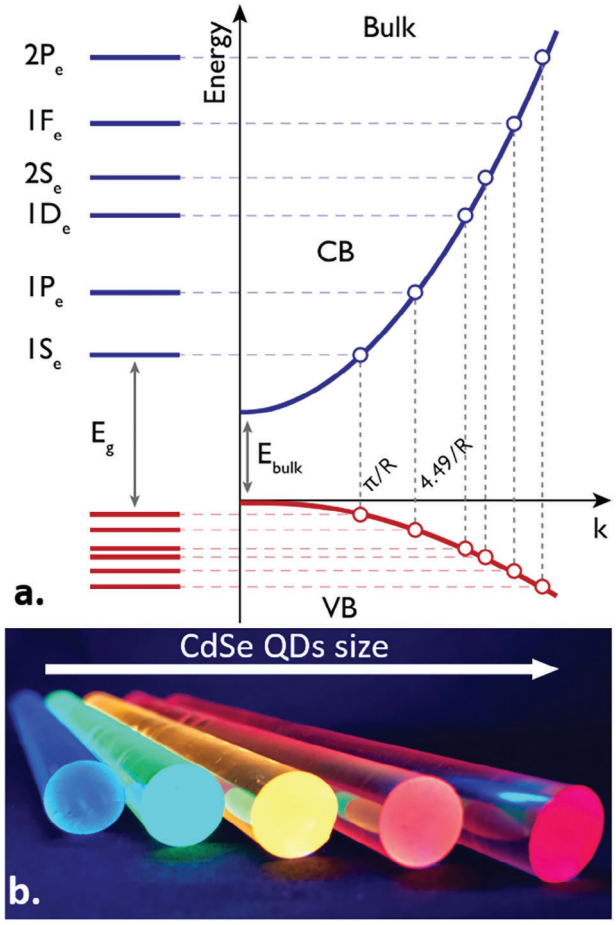

Figure 1. a) Schematized electronic band structure of a semiconductor and its discretization upon confinement. b) Image of plexiglass tubes coated with CdSe NCs of various sizes. The redder the tube, the larger the NCs.

semiconductor platforms. They have proven valuable as biolabels, single photon sources, and particularly as downconverters for wide gamut displays. In such displays, nanocrystals serve as narrow green and red emitters, exemplified in Figure 1b.

Works focusing on other properties of NCs did not arrive until later. Indeed, despite the first successful synthesis of monodisperse colloidal nanocrystals in the early 90s,[1] it took nearly a decade before studies focused on electronic transport in NC arrays were conducted.[2,3] This aspect is crucial to the development of optoelectronic devices based on NCs. This is because the transition from an optically active platform to an optoelectronic one for NCs requires efficient charge conduction inside the NC array, which is a weakly coupled polycrystalline assembly. Making these assemblies conductive has proven to be a difficult challenge.

The main concern for transport inside NC arrays is electronic coupling between individual NCs, since charge transport in these structures occurs thanks to the quantum tunneling of electrons. Paradoxically, the long native ligands from the widely used hot injection method that are responsible for the narrow size distribution also present a significant bottleneck for charge conduction. The extended carbon chains of these capping ligands act as tunnel barriers for the conducting charges, with widths matching the ligand length and heights typically in the range of a few electron volts, depending on the ligand's specific nature. Films of NCs that are capped with these ligands are then not conductive. Early attempts to improve film conductivity thus involved annealing the NC array to remove the native ligands.[2,3] However, this approach presents several issues. First, it causes particle sintering, resulting in a loss of quantum confinement. Additionally, it leaves the surface partially unpassivated, which strongly affects optical properties (band edge energy and sharpness, luminescence efficiency...).[4] Instead of removing ligands, later strategies thus focused on carefully choosing the ligand's size and chemical nature to enhance the particle coupling. Although there have been many attempts to design ligands with conjugated chains,[5–7] the general consensus is that higher coupling is generally obtained with shorter ligands.[8,9]

2. The Mobility Challenge in Nanocrystal Thin Films

Since then, several approaches have been developed to replace the long initial ligands. One approach, known as solid-state ligand exchange (see **Figure 2**), involves a two-step process: depositing nanocrystals onto a substrate and then immersing the film in a solution of shorter ligands. Since the native ligands are labile, they can easily be removed from the surface and replaced by new ligands introduced from the solution. If the new ligands are provided in excess and have a strong affinity for the nanocrystal surface, an efficient ligand exchange can take place. This process can be monitored using infrared spectroscopy by following the drop in absorption of the C—H bonds. Additionally, electrical measurements can be conducted if the ligand exchange occurs directly on a device. As a result of this ligand exchange, a significant increase in the conductivity and photoconductivity of the NC array is generally observed. This improvement in conductivity is primarily attributed to an increase in mobility (μ) as reduced interparticle distance favors charge delocalization. Generally, the mobility increases from an extremely low value in the range of 10^{-8}–10^{-6} cm^2 V^{-1} s^{-1} to ≈10^{-4}-10^{-2} cm^2 V^{-1} s^{-1},[10] as depicted in **Figure 3a**. The final mobility value depends on the completeness of the ligand exchange and the length of the final ligands. Interestingly, even with these relatively low mobilities, a fast photoresponse (i.e., sub-nanosecond) can still be obtained.[11–14]

Despite its potential advantages, this method suffers from certain limitations. One major drawback arises from the diffusive nature of ligand exchange, which is only efficient over short distances. Moreover, as the ligand exchange proceeds, the volume of the nanocrystals is reduced due to the shortening of their ligand shell. This reduction in volume leads to the formation of cracks at a macroscopic level, which is highly detrimental as it results in relatively slow charge percolation between the electrodes. To overcome these issues, a multilayer deposition approach can be employed. However, this technique can quickly become highly time-consuming, especially when aiming to create thick films.

To address the functional limitations of this method and achieve higher mobility values, researchers have introduced inorganic ligands, intending to offer a new level of tunability for the interparticle tunnel barrier by also tuning its height. The concept for this second approach involves exchanging the native ligands for short ions in solution. Although the initial

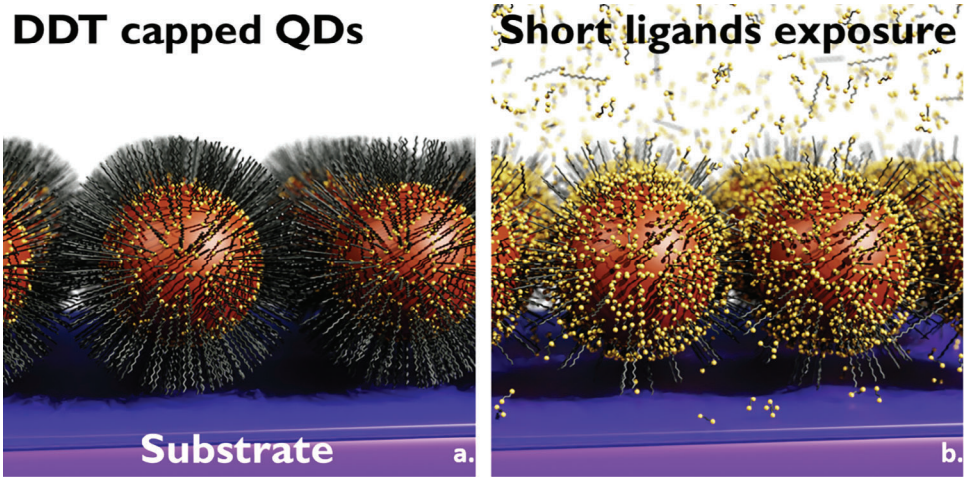

Figure 2. a) Schematic of a nanocrystal array capped with long native ligands and b) capped with shorter ligands after ligand exchange.

procedures were quite complex,[15] they have since been simplified, and a wide range of short ions, such as halides and chalcogenides, have been successfully used.[16–19] As a result, reported mobilities above 1 $cm^2\ V^{-1}\ s^{-1}$ have been achieved,[20,21] with record values reaching a few hundred $cm^2\ V^{-1}\ s^{-1}$.[22] Simultaneously, efforts have been dedicated to creating ordered arrays of necked NCs (mostly PbSe).[23] This area of research has been motivated by the potential applications in designing metamaterials and superlattices. NC superlattices have been studied extensively, wherein nanocrystals self-assemble into superstructures with long-distance coherence.[24] However, in these structures, the nanocrystals typically remain capped by their native ligands, hindering the emergence of electronic coupling. The ordered array of necked nanocrystals, by combining self-assembly with electronic coupling,[25] creates the long-term possibility of inducing new collective properties.[26] Nevertheless, from a mobility perspective, it appears that such necked arrays do not provide significant benefits compared to disordered arrays of the same materials.[27–32]

In the low mobility regime, hopping conduction is the well-established model for conduction in a NC array.[33–35] In this mechanism, charge carriers go from one NC to the next by quantum tunneling. The carrier's wavefunction is delocalized over the individual NC, and the inter-NC medium that creates a tunnel barrier is seen as the bottleneck. As a result, carriers scatter between localized states, and the transfer involves a tradeoff between minimizing the energy of the final state and maximizing the magnitude of the tunneling transmission to this state. The energies at play in this mechanism are:

- The bandgap E_G that determines the thermally activated carrier density
- The disorder energy Δ, which primarily reflects the particle size distribution
- The charging energy E_C, which is the cost to add a charge on a sphere with a given dielectric constant
- The energy drop induced by the application of bias $e\ F\ D$ with e the elementary charge, F the electric field, and D the particle diameter assuming a spherical shape

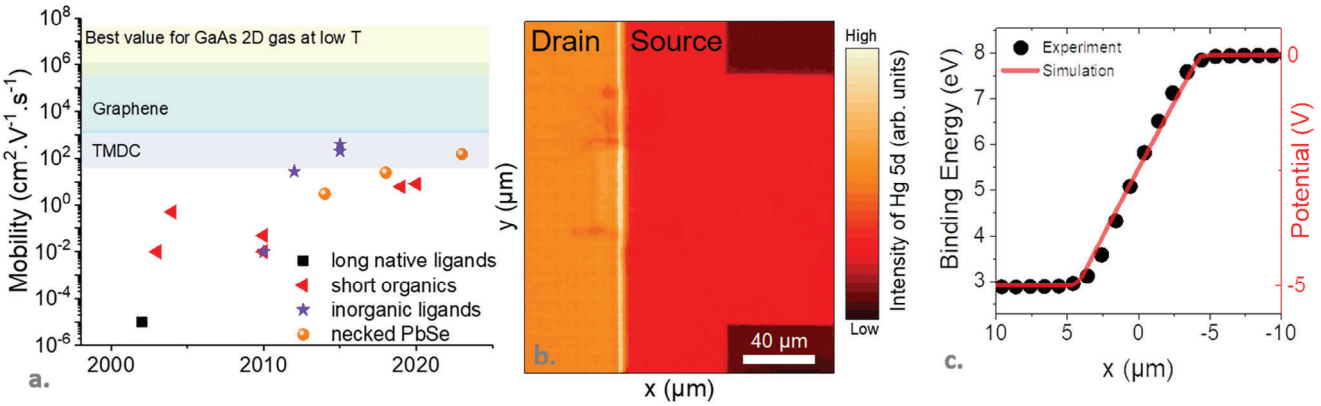

Figure 3. a) Mobility of NC arrays as a function of reported years. NCs have been sorted by surface chemistry (long ligands, short ligands, inorganic ligand, and necked PbSe NCs). b) Photoemission mapping for Hg 5d state coating two electrodes from a field-effect transistor while 5 V bias is applied over the two electrodes. c) The shift of the binding energy of the Hg 5d state in the gap between the two electrodes shows a quasi-linear bias change from one electrode to the other, a behavior consistent with diffusive transport. Figures (b) and (c) are adapted with permission from ref.[36] Copyright {2023} American Chemical Society.

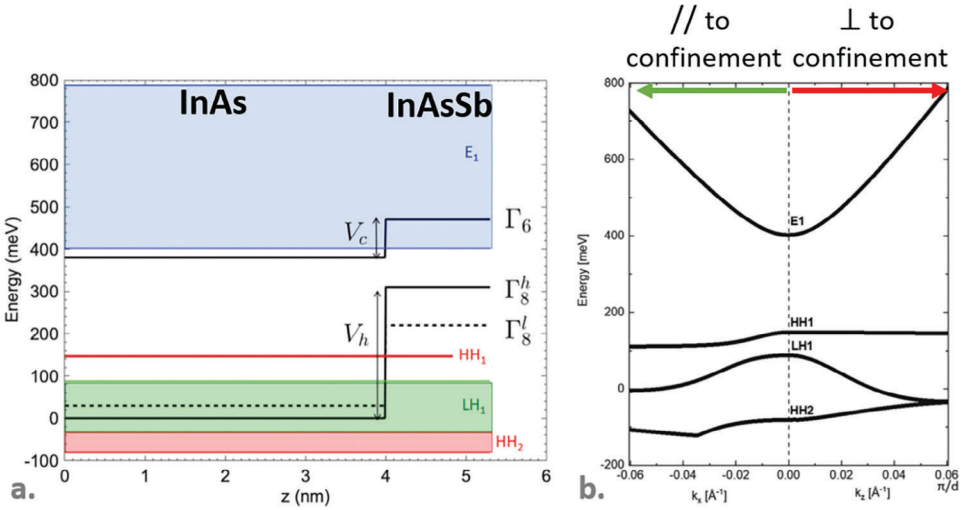

Figure 4. a) Energy profile from an InAs/InAsSb superlattice. Γ_6 depicts the conduction band profile, whereas $\Gamma_{8h/l}$,repectively, the heavy hole and light hole band. In blue is the conduction band miniband, while green and red are the valence band minibands. V_c and V_h depict the band offset between InAs and InAsSb for the conduction and valence band, respectively. b) Calculated energy dispersion along and perpendicular to the confinement. Figures are adapted from ref.[47]

- The thermal energy k_bT with k_b the Boltzmann constant and T the temperature

A recent study utilizing photoemission imaging[36] to map the energy landscape of devices (as shown in Figure 3b) reveals that the bias drop between the electrodes in a nanocrystal-based field-effect transistor follows a quasi-linear trend (as depicted in Figure 3c). This behavior is expected for diffusive transport, in contrast to the case of ballistic transport, where the electric field remains almost null in the bulk of the structure and accumulates at the interface.

3. Competition Between Confinement and Transport

The mechanism governing electronic transport in high-mobility films has been a subject of debate.[37] Particularly, the temperature dependence of the mobility may exhibit a behavior similar to metals, which has been interpreted as a signature of band-like transport.[38–43] This raised significant expectations for further increasing mobility, especially when new high-mobility materials like graphene and transition metal dichalcogenides were also emerging.[44] However, comparing the mobility of NCs with that of 2D materials and the exceptionally high mobility of GaAs 2D electron gas (with μ approaching 10^8 cm^2 V^{-1} s^{-1})[45] is misleading, see Figure 3a. This comparison disregards the influence of quantum confinement, which underlies all the optical properties of NCs. A more appropriate comparison can be made with semiconductor heterostructures, as NCs are gaining popularity in infrared sensing,[46] a field where these heterostructures have been utilized for decades. Quantum well-based heterostructures in semiconductors offer a combination of confinement, for optical design, and efficient charge transport, occurring either within the well or perpendicular to it. By examining transport in both directions, we can directly quantify the "mobility cost" arising from the quantum confinement used to shape the spectral response of the heterostructure. A study on this subject has been conducted with type II superlattices made of InAs/InAsSb heterostructures,[47] as shown in **Figure 4**.

In this study, the Sb content was carefully selected to fulfill two requirements. First, it must maintain a lattice matching with both InAs and the substrate, and second, it must induce a band shift, particularly in the valence band, as illustrated in Figure 4a. Subsequently, electronic dispersion calculations were performed (Figure 4b) parallel and perpendicular to the well direction. Since transport parallel to the well direction is unaffected by quantum confinement, comparing the dispersion between the two directions directly shows the effect of confinement. The conduction band dispersion (labeled E1) is only marginally affected, consistent with the weak conduction band offset. In contrast, the situation for the valence band's ground state exhibits significant differences. Due to the 300 meV offset (a confinement energy similar to what is observed for colloidal NCs in which most values span from 100 to 1000 meV)[48,49] in energy induced by the presence of Sb, holes become confined in the InAsSb layer, leading to a flattening of the band structure. Because the effective mass m^* is a direct measurement of the band curvature $1/\ m^*=\frac{1}{\hbar}\ \frac{\partial^2 E}{\partial k^2}$, a flatter band translates into an increased effective mass. The latter impacts the transport since the mobility is directly connected to the mass through $\mu=\frac{e\tau}{m^*}$ with τ the scattering lifetime (i.e., the equivalent of the hopping time for NC arrays). The authors then calculated that the high mobility of InAsSb (>1000 cm^2 V^{-1} s^{-1} for bulk) results in an "across-heterostructure" mobility of 13.4 cm^2 V^{-1} s $^{-1}$.[50] Notably, this drop in mobility is solely attributable to confinement, as the model neglects any potential imperfections that could further reduce the actual mobility.

The key takeaway from this study is that even when starting from monocrystalline semiconductor films, carefully grown epitaxially, the introduction of 300 meV of confinement leads to a final effective mobility value comparable to the best-reported values for NC arrays. Thus, miniband formation in NC array is

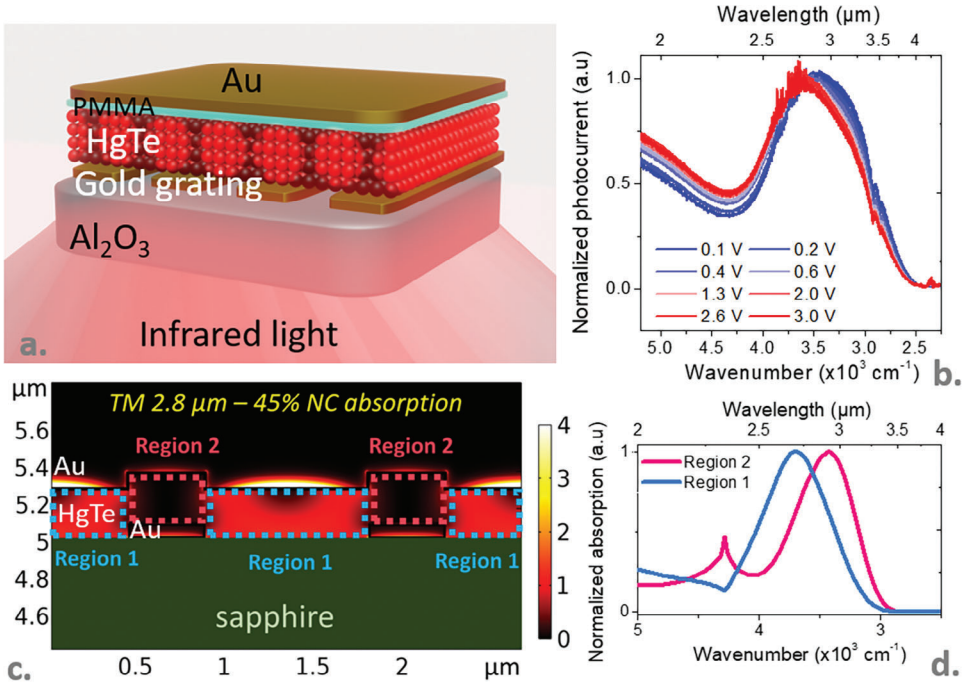

Figure 5. a) Schematic of an infrared NC-based sensor in which the grating acts simultaneously as interdigitated electrodes and as a plasmonic grating. b) Normalized photocurrent spectra under various applied biases. c) Simulated absorption map in TM polarization at 2.8 μm for the device depicted in part a. d) Simulated absorption spectra for the two regions of the device as depicted in part (c). Region 1 (between electrodes) is blue-shifted compared to region 2 (on top of gold grating). Figure is adapted with permission from ref. [60]. Copyright {2021} American Chemical Society.

unlikely to increase significantly the carrier mobility, given their higher disorder. Therefore, efforts should be focused on the benefit of hopping and associated properties that cannot be achieved using epitaxially grown material. Our belief is that hopping can be crucial in rendering NC-based devices active, particularly in bias reconfigurable applications, as the field of active photonics is driven by mechanical resonators (the so-called MEMS)[51] and phase change materials (Ge-based chalcogenides).[52,53] In the last part of this discussion, we thus focus on how the properties of hopping transport have been utilized to introduce novel ways of reconfiguring spectral responses with bias in NC-based devices.

4. Bias-Reconfigurable Optical Modulation with Nanocrystal Thin Films

The typical method to induce spectral tunability through the application of bias in semiconductors is achieved using the Stark effect.[54] Under an electric field, the effective bandgap is reduced, resulting in a redshift of the spectral response. This effect is commonly used in designing light modulators by applying electric fields of ≈100 kV cm^{-1}. In NCs, a similar effect is observed,[55–58] and this fundamental observation has sparked interest in using NCs as trackers of neuron activity.[59] However, the practical use of this effect is limited due to the relatively large electric field required for its observation. Therefore, exploring alternative strategies to achieve field-induced reconfigurability is of great interest.

Recently Dang et al.[60] observed in a device dedicated to infrared sensing (**Figure 5a**) a spectral shift of the photocurrent spectrum with applied bias. Surprisingly, the observed shift was a blueshift (Figure 5b), while the Stark effect typically leads to a redshift of the response. Although the magnitude of the shift was modest and smaller than the exciton linewidth, it was still observable even at weak electric fields of ≈15 kV.cm^{-1} (i.e., corresponding to 8 mV drop over a 5 nm NC which stays very small compared to its bandgap). Since this phenomenon cannot be attributed to the Stark effect, and it is not observed in a bare NC film, the origin of the reconfigurable response is attributed to the use of a light resonator. In the device shown in Figure 5a, the grating serves a dual purpose: it acts both as interdigitated electrodes and as a plasmonic grating. The period of the plasmonic grating is chosen to generate resonances, with the wavelength of resonance almost matching the band edge of the NCs. Originally, the plasmonic cavity was intended to enhance light absorption by focusing the light over a slab of NCs with a thickness more compatible with the limited diffusion length. However, the presence of the resonator also induces an inhomogeneous distribution in the absorption map, as illustrated in Figure 5c. A cavity is formed between the grating stripes and the top gold layer of the device. Inside the cavity (region 2 in Figure 5c), the resonance of the cavity leads to a different absorption spectrum of the NCs than outside (region 1): the absorption spectrum is red-shifted (Figure 5d) in region 2 compared to region 1.

Then, hopping comes into play! Indeed, the mechanism of hopping transport plays a crucial role in how this difference of inhomogeneous absorption leads to a bias-reconfigurable response.[61] **Figure 6a** illustrates a schematized hopping transport in various situations, ranging from a monodisperse population with no applied field to a polydisperse size distribution in the presence of an electric field.

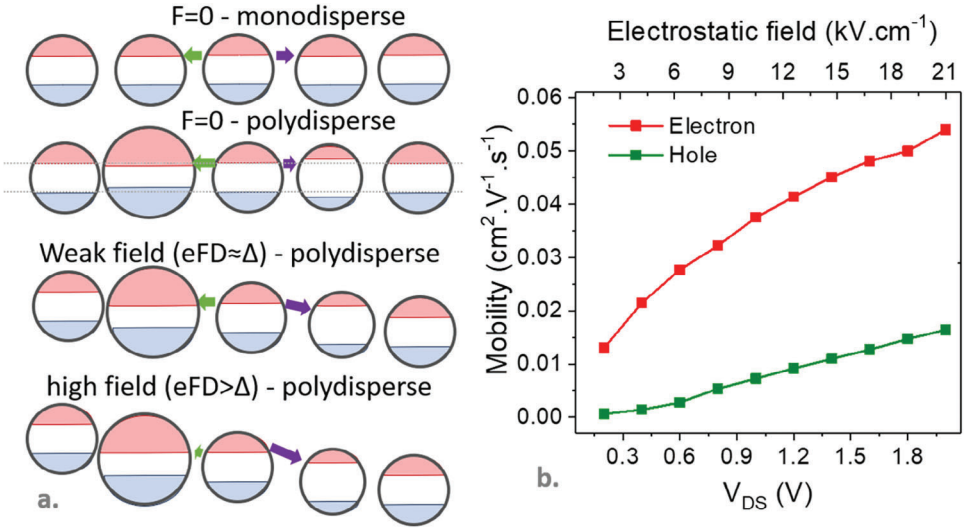

Figure 6. a) Schematic of an NC array energy profile in different situations. From top to bottom: no electric field is applied and size distribution is monodisperse; no electric field is applied and size distribution is polydisperse; a weak field is applied and size distribution is polydisperse; a large electric field is applied and size distribution is polydisperse. b) Measured electron and hole mobilities from an HgTe NC array as a function of the applied bias voltage. Part (b) is adapted with permission from ref. [71]. Copyright {2022} American Chemical Society.

In the absence of a field and for monodisperse NCs, carrier movement follows a random walk with no preferential direction, resulting in a zero global current. In a more realistic model, when the size distribution is polydisperse, quantum confinement leads to a distribution of band edge energies. Larger NCs, which are less confined, have a reduced bandgap and effectively act as traps in the low carrier density limit.[62,63] Conversely, if the NC array becomes charged (through gating,[10] doping,[9] or self-doping[64–66]), the larger dots are the first to become fully filled, rendering them inactive for transport and making the percolation path more tortuous.

Once an electric field (F) is applied, a bias drop occurs across the NC, resulting in a net current. We can introduce an energy term Δ that represents the energy disorder induced by the size distribution. With this term, we can define a weak field limit, when the drop in energy between two adjacent nanocrystals (e F D) remains of the same magnitude as Δ. In a 3D NC array, carriers follow a complex pathway where the location of the next hop is determined by which adjacent NC has the lowest energy. In the weak field limit, the energy can be minimized either by following the potential drop induced by the applied field or by going to a particle with a bigger size and a reduced confinement, since the difference in energy gained from both these choices is equivalent. Consequently, transport does not necessarily occur along the field direction, and a diffusive 3D path is followed with a less effective pathway. This diffusive behavior is characterized by the diffusion length L_D, which is related to the carrier lifetime τ through $L_D\,(F,T) = \sqrt{D_0(F,T)\cdot\tau}$. When the magnitude of the field is increased and reaches the limit where e F D > Δ, it becomes more favorable to minimize energy by following the bias drop rather than following a perpendicular pathway along the direction of weaker confinement. In other words, transport becomes less diffusive, and fewer hopping steps are required to transport charges from one electrode to the other.[67] In this field-assisted hopping transport,[68] the diffusion coefficient can be described by an effective model $D(F,T) = D_0(T)+A(F,T)\ F^2$,[69,70] where $D_0(T)$ is the diffusion coefficient in the zero-field limit, F is the magnitude of the electric field, and $A(F,T)$ is a coupling factor. This increase in the diffusion coefficient translates macroscopically into a rise in carrier mobility. In other words, mobility is higher under a higher applied bias, as observed experimentally in Figure 6b, and the diffusion length is bias-dependent.

We can now understand the bias-induced shift of the photocurrent spectra (Figure 5b) thanks to a combination of inhomogeneous absorption mapping and bias-dependent diffusion length. At low bias, charge collection near the electrode is favored, making the spectral response similar to the mode located close to the electrode (defined as Region 2 in Figure 5c). The absorption in this mode is driven by the metal-dielectric-metal cavity defined between the grating stripes and the top metal layer. This mode appears slightly redshifted compared to the response of the material away from the electrode (Figure 5d and Region 1 in Figure 5c). When the field is increased, charge collection away from the electrode gains relative weight, and the photocurrent spectrum becomes more similar to the absorption away from the vertical cavity.

5. Application to Active Photonic Devices

Now, coming back to the basic design of bias-reconfigurable NC-based photonic structures, we can say that bias-reconfigurability is a combination of two factors: i) spatially inhomogeneous absorption and ii) bias-dependent mobility/diffusion length, which appears to be an intrinsic property of NC arrays. However, to utilize bias dependence effectively, the device characteristic length must roughly match the diffusion length. This explains why such bias dependency is not observed in most planar devices based on NCs, where the electrode spacing is generally above 1 µm, significantly exceeding the diffusion length. Concerning vertical diodes, in which the device length matches this condition, the

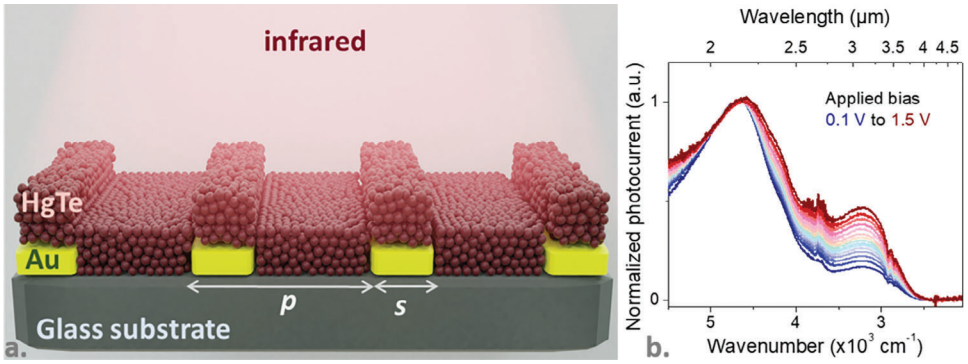

Figure 7. a) Schematic of a gold grating deposited on glass and coated with a NC film. b) Normalized photocurrent spectra under various applied bias voltages for the device depicted in part (a). Figures are adapted with permission from ref. [71] Copyright {2022} American Chemical Society.

absorption is generally spatially homogeneous. The spatial shaping of the electromagnetic field inside the device can be achieved by introducing a photonic cavity to the structure. A plasmonic grating is resonant for a period $p \approx \lambda/n$, with λ being the resonance wavelength and n the refractive index. In NC films, the refractive index ranges from 2 to 3 depending on the material[72] and particularly on the surface chemistry and packing.[73,74] The more efficient the ligand exchange, the higher the refractive index. Similarly, the use of a Fabry-Perot cavity will lead to a cavity size L with a scaling of $\lambda/2n$. The consequence of such scaling is that targeting longer wavelengths requires larger structures, and their size may become larger than the diffusion length. This is certainly why this approach has been successful mostly in the near and short-wave infrared regions. This strategy can be extended toward shorter wavelengths, especially in the visible range.[60,71,75] However, in this case, where smaller structures are required, the challenge lies in the nanofabrication: the smaller the structure, the harder they are to fabricate.

To confirm that the two key ingredients contributing to a bias-tunable response are indeed the combination of an inhomogeneous absorption map and a bias-dependent diffusion length resulting from hopping, Dang et al.[71] proposed a second structure, as shown in **Figure** 7a. While their initial structure was primarily designed to enhance the absorption magnitude, the second one was made to enhance the spatial inhomogeneity of the absorption map. The second significant advantage of this structure is its simplicity. The device consists of interdigitated gold electrodes on glass, coated with a film of NCs. Such a structure aligns with the most conventional device geometry for conducting transport in an NC array. The critical choice here lies in the geometrical factors that enable the bias reconfigurability of the response. The device encompasses two electromagnetic modes: a plasmonic mode generated by the metal grating, whose resonant wavelength is determined by the grating period, and a planar Fabry-Perot cavity arising from the index mismatch between the NC film on top of the glass and the same material on top of the metal. Consequently, the film between the electrodes acts as a horizontal cavity. The grating period (p) and digit size (s) are chosen to ensure that both modes are not only spatially separate but also spectrally distinct (appearing at 2.3 and 3.2 μm, as seen in Figure 7b). This modified device now exhibits a significantly enhanced bias reconfigurability compared to the previous case,[71] as depicted in Figure 5b. Instead of just a small spectral shift, the relative magnitudes of the two electromagnetic modes in the photocurrent spectra can be altered by a factor of 2. Furthermore, whereas the previous shift was only observed at cryogenic temperatures (i.e., below 120 K), the bias tunability is now maintained up to almost room temperature.

The two previous structures rely on a continuous film of NCs functionalizing a grating. This configuration makes the electromagnetic modes leaky, which limits their spatial separation. To further enhance the spatial inhomogeneity of the electromagnetic field, Dang et al.[75] later proposed a new periodic structure with two patterns per period, and two different spacings, as shown in **Figure** 8a. The grating is still used as an interdigitated electrode to enable planar photoconduction. Each interelectrode medium acts as a cavity and the generated resonances have very weak spatial overlap. The spectral responses of each of these cavities are depicted in Figure 8b. At low bias, the photocurrent spectrum corresponds to the absorption from the large groove only, as shown in Figure 8c. This is due to the larger amount of NCs in this region, leading to stronger absorption compared to the small groove. When the bias is increased, the absorption of the small groove gains spectral weight: due to the smaller distance between electrodes, the applied field is larger compared to the large groove and charge transport becomes more efficient. By applying very limited bias voltages (up to 1 V), the spectral weight of the small groove can be modulated on and off by a factor of 50, as seen in the inset of Figure 8c. An important question left unaddressed is the speed of modulation, which can be critical with the use of such component as a modulator in mind. Nevertheless the planar character of the latest devices tends to reduce their capacitance which probably favors high speed modulation.

These works open up the possibility for an actively reconfigurable photoresponse in NC-based devices. Contrasting with the common strategies of achieving spectral tunability through geometrical adjustments (particle size, resonator geometry), these works create possibilities for integrating active filters at the chip level. Certainly, as one of the goals of using infrared NCs is cost disruption, it is critical to achieve competitive costs not only in the NC growth compared to epitaxial growth, but also in the entire packaging of the final device. Further cost reductions can be anticipated by integrating optical functions at the chip level. Another benefit of this response reconfigurability is its ability to prevent the use of countermeasures to the detectors. A typical method to disturb the observation of an infrared scene is to

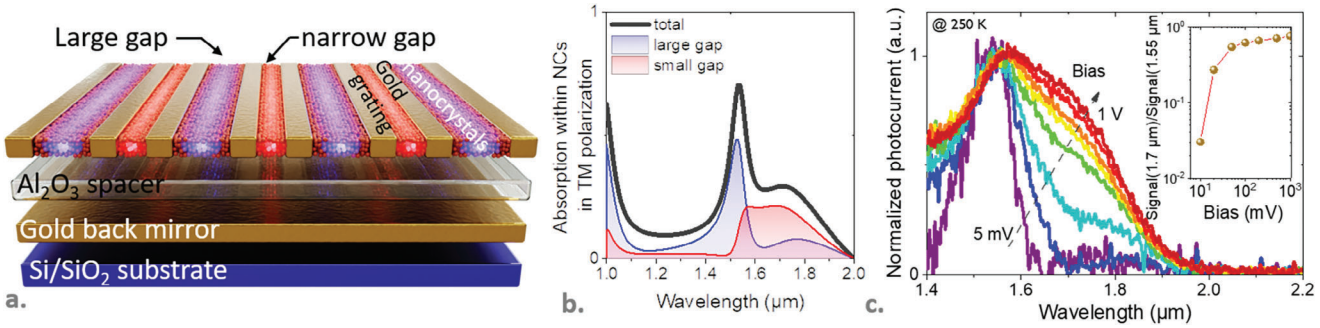

Figure 8. a)Schematic of a two pattern per period (with one gap of 200 nm and the other being 400 nm wide) grating coated with infrared NCs. b) Simulated absorption spectra for the total structure depicted in part a and each gap. c) Normalized photocurrent spectra under various applied biases show that the response of the small gap can be turned on and off. The inset provides the bias dependence of the photocurrent ratio at 1.7 μm (narrow groove) and at 1.55 μm (corresponding to the large groove). Figure is adapted with permission from ref. [75] Copyright {2023} American Chemical Society.

blur the sensor using a laser. Here, we demonstrate that photoresponse can be reduced over narrow spectral lines matching conventional countermeasure wavelengths (1.064, 1.55, 10.6 μm...). This makes these reconfigurable devices capable of operating even if countermeasures are activated.

6. Conclusion

Hopping conduction and its inherent limited mobility have long been regarded as a bottleneck for the optoelectronic integration of NCs, which was expected to prevent the handling of high currents or achieve rapid current modulation. However, both of these objectives have now been realized in LEDs,[76] and infrared sensors,[11–14] respectively. Additionally, through surface chemistry modifications, mobility values (≈10 $cm^2.V^{-1}.s^{-1}$) have approached those achieved in epitaxially grown heterostructures that include quantum confinement. Therefore, hopping should instead be regarded as an opportunity to generate novel properties that cannot be attained in semiconductors featuring ballistic transport. One of these properties is the bias-dependent diffusion length, which, when coupled with a thoughtfully designed electromagnetic field, enables the active reconfigurability of the spectral response–a realm where NCs had not been previously involved. Over a few years, the concept of this bias-tunable response has evolved from observing marginal spectral shifts to attaining the full capability to switch the response on and off within a specific spectral range. Now, there is a need to expand the potential of the filtering function, broaden the spectral range in which they can operate, and ultimately extend the concept toward integration into a complete imaging system.

Acknowledgements

Authors thank Maxime Bouschet, Robson Ferreira, Francesca Carosella for insightful discussions. The project is supported by ERC grants blackQD (grant no. 756225), Ne2dem (grant 853049), and AQDtive (grant no. 101086358). This work was supported by French state funds managed by the Agence Nationale de la recherche (ANR) through the grant Copin (ANR-19-CE24-0022), Frontal (ANR-19-CE09-0017), Graskop (ANR-19-CE09-0026), NITQuantum (ANR-20-ASTR-0008), Bright (ANR-21-CE24-0012), MixDFerro (ANR-21-CE09-0029), Quicktera (ANR-22-CE09-0018), Operatwist (ANR-22-CE09-0037-01) and E-map(ANR-23-CE). This project has received financial support from the CNRS through the MITI interdisciplinary programs (project within).

Conflict of Interest

The authors declare no conflict of interest.

Keywords

active photonic, electronic transport, hopping conduction, infrared sensors, nanocrystals

Received: September 4, 2023
Revised: November 26, 2023
Published online:

[1] C. B. Murray, D. J. Norris, M. G. Bawendi, *J. Am. Chem. Soc.* **1993**, *115*, 8706.
[2] M. Drndic, M. V. Jarosz, N. Y. Morgan, M. A. Kastner, M. G. Bawendi, *J. Appl. Phys.* **2002**, *92*, 7498.
[3] C. A. Leatherdale, C. R. Kagan, N. Y. Morgan, S. A. Empedocles, M. A. Kastner, M. G. Bawendi, *Phys. Rev. B* **2000**, *62*, 2669.
[4] J. Yuan, L. Hu, Z. Xu, Y. Zhang, H. Li, X. Cao, H. Liang, S. Ruan, Y.-J. Zeng, *J. Phys. Chem. C* **2019**, *123*, 14766.
[5] P. Reiss, E. Couderc, J. De Girolamo, A. Pron, *Nanoscale* **2011**, *3*, 446.
[6] S. Bhattacharyya, A. Patra, *J. Photochem. Photobiol., C* **2014**, *20*, 51.
[7] Y.-W. Su, W.-H. Lin, Y.-J. Hsu, K.-H. Wei, *Small* **2014**, *10*, 4427.
[8] Y. Liu, M. Gibbs, J. Puthussery, S. Gaik, R. Ihly, H. W. Hillhouse, M. Law, *Nano Lett.* **2010**, *10*, 1960.
[9] D. Yu, C. Wang, P. Guyot-Sionnest, *Science* **2003**, *300*, 1277.
[10] D. V. Talapin, C. B. Murray, *Science* **2005**, *310*, 86.
[11] J. Gao, A. F. Fidler, V. I. Klimov, *Nat. Commun.* **2015**, *6*, 8185.
[12] B. Martinez, C. Livache, N. Goubet, A. Jagtap, H. Cruguel, A. Ouerghi, E. Lacaze, M. G. Silly, E. Lhuillier, *J. Phys. Chem. C* **2018**, *122*, 859.
[13] A. Maier, F. Strauß, P. Kohlschreiber, C. Schedel, K. Braun, M. Scheele, *Nano Lett.* **2022**, *22*, 2809.
[14] C. Livache, N. Goubet, B. Martinez, A. Jagtap, J. Qu, S. Ithurria, M. G. Silly, B. Dubertret, E. Lhuillier, *ACS Appl. Mater. Interfaces* **2018**, *10*, 11880.
[15] M. V. Kovalenko, M. Scheele, D. V. Talapin, *Science* **2009**, *324*, 1417.

[16] J. Tang, K. W. Kemp, S. Hoogland, K. S. Jeong, H. Liu, L. Levina, M. Furukawa, X. Wang, R. Debnath, D. Cha, K. W. Chou, A. Fischer, A. Amassian, J. B. Asbury, E. H. Sargent, *Nat. Mater.* **2011**, *10*, 765.
[17] A. Nag, M. V. Kovalenko, J.-S. Lee, W. Liu, B. Spokoyny, D. V. Talapin, *J. Am. Chem. Soc.* **2011**, *133*, 10612.
[18] D. S. Dolzhnikov, H. Zhang, J. Jang, J. S. Son, M. G. Panthani, T. Shibata, S. Chattopadhyay, D. V. Talapin, *Science* **2015**, *347*, 425.
[19] E. Talgorn, Y. Gao, M. Aerts, L. T. Kunneman, J. M. Schins, T. J. Savenije, M. A. Van Huis, H. S. J. Van Der Zant, A. J. Houtepen, L. D. A. Siebbeles, *Nat. Nanotechnol.* **2011**, *6*, 733.
[20] D. M. Balazs, B. M. Matysiak, J. Momand, A. G. Shulga, M. Ibáñez, M. V. Kovalenko, B. J. Kooi, M. A. Loi, *Adv. Mater.* **2018**, *30*, 1802265.
[21] Y. Liu, J. Tolentino, M. Gibbs, R. Ihly, C. L. Perkins, Y. Liu, N. Crawford, J. C. Hemminger, M. Law, *Nano Lett.* **2013**, *13*, 1578.
[22] J. Jang, D. S. Dolzhnikov, W. Liu, S. Nam, M. Shim, D. V. Talapin, *Nano Lett.* **2015**, *15*, 6309.
[23] W. H. Evers, B. Goris, S. Bals, M. Casavola, J. De Graaf, R. Van Roij, M. Dijkstra, D. Vanmaekelbergh, *Nano Lett.* **2013**, *13*, 2317.
[24] C. B. Murray, C. R. Kagan, M. G. Bawendi, *Science* **1995**, *270*, 1335.
[25] I. Coropceanu, E. M. Janke, J. Portner, D. Haubold, T. D. Nguyen, A. Das, C. P. N. Tanner, J. K. Utterback, S. W. Teitelbaum, ¸ M. H. Hudson, N. A. Sarma, A. M. Hinkle, C. J. Tassone, A. Eychmüller, D. T. Limmer, M. Olvera De La Cruz, N. S. Ginsberg, D. V. Talapin, *Science* **2022**, *375*, 1422.
[26] C. R. Kagan, C. B. Murray, *Nat. Nanotechnol.* **2015**, *10*, 1013.
[27] C. S. S. Sandeep, J. M. Azpiroz, W. H. Evers, S. C. Boehme, I. Moreels, S. Kinge, L. D. A. Siebbeles, I. Infante, A. J. Houtepen, *ACS Nano* **2014**, *8*, 11499.
[28] M. P. Boneschanscher, W. H. Evers, J. J. Geuchies, T. Altantzis, B. Goris, F. T. Rabouw, S. A. P. Van Rossum, H. S. J. Van Der Zant, L. D. A. Siebbeles, G. Van Tendeloo, I. Swart, J. Hilhorst, A. V. Petukhov, S. Bals, D. Vanmaekelbergh, *Science* **2014**, *344*, 1377.
[29] W. H. Evers, J. M. Schins, M. Aerts, A. Kulkarni, P. Capiod, M. Berthe, B. Grandidier, C. Delerue, H. S. J. Van Der Zant, C. Van Overbeek, J. L. Peters, D. Vanmaekelbergh, L. D. A. Siebbeles, *Nat. Commun.* **2015**, *6*, 8195.
[30] M. Zhao, F. Yang, C. Liang, D. Wang, D. Ding, J. Lv, J. Zhang, W. Hu, C. Lu, Z. Tang, *Adv. Funct. Mater.* **2016**, *26*, 5182.
[31] V. Notot, W. Walravens, M. Berthe, N. Peric, A. Addad, X. Wallart, C. Delerue, Z. Hens, B. Grandidier, L. Biadala, *ACS Nano* **2022**, *16*, 3081.
[32] J. Pinna, R. Mehrabi Koushki, D. S. Gavhane, M. Ahmadi, S. Mutalik, M. Zohaib, L. Protesescu, B. J. Kooi, G. Portale, M. A. Loi, *Adv. Mater.* **2023**, *35*, 2207364.
[33] P. Guyot-Sionnest, *J. Phys. Chem. Lett.* **2012**, *3*, 1169.
[34] N. Prodanovic, N. Vukmirovic, Z. Ikonic, P. Harrison, D. Indjin, *J. Phys. Chem. Lett.* **2014**, *5*, 1335.
[35] V. I. Arkhipov, H. Bässler, *Philos. Mag. Lett.* **1993**, *67*, 343.
[36] M. Cavallo, E. Bossavit, H. Zhang, C. Dabard, T. H. Dang, A. Khalili, C. Abadie, R. Alchaar, D. Mastrippolito, Y. Prado, L. Becerra, M. Rosticher, M. G. Silly, J. K. Utterback, S. Ithurria, J. Avila, D. Pierucci, E. Lhuillier, *Nano Lett.* **2023**, *23*, 1363.
[37] M. Scheele, *Z. Phys. Chem.* **2015**, *229*, 167.
[38] K. V. Reich, T. Chen, B. I. Shklovskii, *Phys. Rev. B* **2014**, *89*, 235303.
[39] K. V. Reich, B. I. Shklovskii, *Appl. Phys. Lett.* **2016**, *108*, 113104.
[40] K. Whitham, J. Yang, B. H. Savitzky, L. F. Kourkoutis, F. Wise, T. Hanrath, *Nat. Mater.* **2016**, *15*, 557.
[41] S. Xu, D. Thian, S. Wang, Y. Wang, F. B. Prinz, *Phys. Rev. B* **2014**, *90*, 144202.
[42] J.-H. Choi, A. T. Fafarman, S. J. Oh, D.-K. Ko, D. K. Kim, B. T. Diroll, S. Muramoto, J. G. Gillen, C. B. Murray, C. R. Kagan, *Nano Lett.* **2012**, *12*, 2631.
[43] J.-S. Lee, M. V. Kovalenko, J. Huang, D. S. Chung, D. V. Talapin, *Nat. Nanotechnol.* **2011**, *6*, 348.
[44] L. A. Ponomarenko, R. Yang, T. M. Mohiuddin, M. I. Katsnelson, K. S. Novoselov, S. V. Morozov, A. A. Zhukov, F. Schedin, E. W. Hill, A. K. Geim, *Phys. Rev. Lett.* **2009**, *102*, 206603.
[45] Y. J. Chung, A. Gupta, K. W. Baldwin, K. W. West, M. Shayegan, L. N. Pfeiffer, *Phys. Rev. B* **2022**, *106*, 075134.
[46] Y. Tian, H. Luo, M. Chen, C. Li, S. V. Kershaw, R. Zhang, A. L. Rogach, *Nanoscale* **2023**, *15*, 6476.
[47] G. Krizman, F. Carosella, J. Bermejo-Ortiz, A. Philippe, J. B. Rodriguez, J.-P. Perez, P. Christol, L.-A. De Vaulchier, Y. Guldner, *J. Appl. Phys.* **2021**, *130*, 055704.
[48] M. A. Hines, G. D. Scholes, *Adv. Mater.* **2003**, *15*, 1844.
[49] B. T. Diroll, B. Guzelturk, H. Po, C. Dabard, N. Fu, L. Makke, E. Lhuillier, S. Ithurria, *Chem. Rev.* **2023**, *123*, 3543.
[50] V. Arounassalame, M. Bouschet, R. Alchaar, R. Ferreira, F. Carosella, A. Ramiandrasoa, J. P. Perez, N. Péré-Laperne, P. Christol, I. Ribet-Mohamed, *Infrared Phys. Technol.* **2022**, *126*, 104315.
[51] T. Stark, M. Imboden, S. Kaya, A. Mertiri, J. Chang, S. Erramilli, D. Bishop, *ACS Photonics* **2016**, *3*, 14.
[52] X. Shi, C. Chen, S. Liu, G. Li, *Nanomaterials* **2020**, *10*, 2530.
[53] A. V. Pogrebnyakov, J. A. Bossard, J. P. Turpin, J. D. Musgraves, H. J. Shin, C. Rivero-Baleine, N. Podraza, K. A. Richardson, D. H. Werner, T. S. Mayer, *Opt. Mater. Express* **2018**, *8*, 2264.
[54] D. A. B. Miller, D. S. Chemla, T. C. Damen, A. C. Gossard, W. Wiegmann, T. H. Wood, C. A. Burrus, *Phys. Rev. Lett.* **1984**, *53*, 2173.
[55] S. A. Empedocles, M. G. Bawendi, *Science* **1997**, *278*, 2114.
[56] R. Scott, A. W. Achtstein, A. V. Prudnikau, A. Antanovich, L. D. A. Siebbeles, M. Artemyev, U. Woggon, *Nano Lett.* **2016**, *16*, 6576.
[57] E. J. D. Klem, L. Levina, E. H. Sargent, *Appl. Phys. Lett.* **2005**, *87*, 053101.
[58] G. Walters, M. Wei, O. Voznyy, R. Quintero-Bermudez, A. Kiani, D.-M. Smilgies, R. Munir, A. Amassian, S. Hoogland, E. Sargent, *Nat. Commun.* **2018**, *9*, 4214.
[59] A. L. Efros, J. B. Delehanty, A. L. Huston, I. L. Medintz, M. Barbic, T. D. Harris, *Nat. Nanotechnol.* **2018**, *13*, 278.
[60] T. H. Dang, A. Vasanelli, Y. Todorov, C. Sirtori, Y. Prado, A. Chu, C. Gréboval, A. Khalili, H. Cruguel, C. Delerue, G. Vincent, E. Lhuillier, *Nano Lett.* **2021**, *21*, 6671.
[61] H. Lepage, A. Kaminski-Cachopo, A. Poncet, G. Le Carval, *J. Phys. Chem. C* **2012**, *116*, 10873.
[62] N. Yazdani, S. Andermatt, M. Yarema, V. Farto, M. H. Bani-Hashemian, S. Volk, W. M. M. Lin, O. Yarema, M. Luisier, V. Wood, *Nat. Commun.* **2020**, *11*, 2852.
[63] S. Volk, N. Yazdani, O. Yarema, M. Yarema, V. Wood, *ACS Appl. Electron. Mater.* **2020**, *2*, 398.
[64] A. Jagtap, C. Livache, B. Martinez, J. Qu, A. Chu, C. Gréboval, N. Goubet, E. Lhuillier, *Opt. Mater. Express* **2018**, *8*, 1174.
[65] K. S. Jeong, Z. Deng, S. Keuleyan, H. Liu, P. Guyot-Sionnest, *J. Phys. Chem. Lett.* **2014**, *5*, 1139.
[66] J. Kim, D. Choi, K. S. Jeong, *Chem. Commun.* **2018**, *54*, 8435.
[67] Y. Xing, N. Yazdani, W. M. M. Lin, M. Yarema, R. Zahn, V. Wood, *ACS Appl. Electron. Mater.* **2022**, *4*, 631.
[68] R. N. Pereira, S. Niesar, W. B. You, A. F. Da Cunha, N. Erhard, A. R. Stegner, H. Wiggers, M.-G. Willinger, M. Stutzmann, M. S. Brandt, *J. Phys. Chem. C* **2011**, *115*, 20120.
[69] A. V. Nenashev, F. Jansson, S. D. Baranovskii, R. Österbacka, A. V. Dvurechenskii, F. Gebhard, *Phys. Rev. B* **2010**, *81*, 115204.
[70] A. V. Nenashev, F. Jansson, S. D. Baranovskii, R. Österbacka, A. V. Dvurechenskii, F. Gebhard, *Phys. Rev. B* **2010**, *81*, 115203.
[71] T. H. Dang, A. Khalili, C. Abadie, C. Gréboval, M. Cavallo, H. Zhang, E. Bossavit, J. K. Utterback, E. Dandeu, Y. Prado, G. Vincent, S. Ithurria,

Y. Todorov, C. Sirtori, A. Vasanelli, E. Lhuillier, *ACS Photonics* **2022**, *9*, 2528.
[72] P. Rastogi, A. Chu, T. H. Dang, Y. Prado, C. Gréboval, J. Qu, C. Dabard, A. Khalili, E. Dandeu, B. Fix, X. Z. Xu, S. Ithurria, G. Vincent, B. Gallas, E. Lhuillier, *Adv. Opt. Mater.* **2021**, *9*, 2002066.
[73] B. Chehaibou, C. Abadie, Y. Prado, X. Z. Xu, G. Vincent, B. Gallas, G. Mugny, A. Arnaud, E. Lhuillier, C. Delerue, *J. Phys. Chem. C* **2023**, *127*, 13789.
[74] B. Chehaibou, E. Izquierdo, A. Chu, C. Abadie, M. Cavallo, A. Khalili, T. H. Dang, C. Gréboval, X. Z. Xu, S. Ithurria, G. Vincent, B. Gallas, G. Mugny, A. Arnaud, E. Lhuillier, C. Delerue, *Nanoscale* **2022**, *14*, 2711.
[75] T. H. Dang, C. Abadie, A. Chu, M. Cavallo, A. Khalili, C. Dabard, E. Bossavit, H. Zhang, Y. Prado, D. Pierucci, J. K. Utterback, Y. Todorov, C. Sirtori, J. Jaeck, G. Vincent, A. Vasanelli, B. Fix, E. Lhuillier, *ACS Photonics* **2023**, *10*, 1601.
[76] H. Jung, Y.-S. Park, N. Ahn, J. Lim, I. Fedin, C. Livache, V. I. Klimov, *Nat. Commun.* **2022**, *13*, 3734.

Nicolas Ledos graduated from the University of Angers with a master's degree in Organic Electronics in 2018. He received his Ph.D. in chemistry in 2022 from the University of Rennes. During his Ph.D., his work focused on the development of organophosphorus π-conjugated systems for light-emitting diodes. He then joined the group of Emmanuel Lhuillier at INSP (Paris) as a postdoctoral researcher in 2023. His current research mainly focuses on the development of optoelectronic devices for infrared detection based on HgTe nanocrystals.

Tung H. Dang received his B.S in physics (2017) from Vietnam National University, Hanoi, and his M.S in condensed matter physics from Université Paris-Saclay and ENS Paris (2020). He obtained a Ph.D. degree in 2023 from Université Paris-Cité under the supervision of Angela Vasanelli and Emmanuel Lhuillier. His work involved using optical and plasmonic resonators to improve the performance of infrared photodetectors based on colloidal quantum dots. He is now post doc in los Alamos national lab working in V. Klimov group.

Mariarosa Cavallo is a PhD student in Physics and Chemistry of Materials at Sorbonne University, under the supervision of Emmanuel Lhuillier. Her research focuses on the characterization of colloidal narrow bandgap nanocrystals for infrared optoelectronics.

Huichen Zhang is a third-year Ph.D. student at Sorbonne University under the supervision of Emmanuel Lhuillier. She received a bachelor's degree from Nanjing University of Science and Technology and a master's from Nanjing University in China. She is interested in nanocrystal synthesis for infrared optoelectronic devices.

Erwan Bossavit is a PhD student in a joint project between the INSP laboratory of Sorbonne Université and the SOLEIL synchrotron, supervised by E. Lhuillier and M.G. Silly. His research interests revolve around the design and implementation of novel infrared-emitting LEDs based on nanocrystals.

Adrien Khalili is a postdoctoral researcher at Institut des Nanosciences de Paris, Sorbonne Université. He received his master's degree in applied physics from Ecole Normale Supérieur Paris-Saclay and completed his Ph.D. at Sorbonne Université, focusing on the optoelectronics of infrared nanocrystals. His current research is centered on advancing nanocrystal-based infrared camera technology.

Lam Nguyen Do holds an MSc degree in Display Engineering from Hoseo University, South Korea. Currently pursuing a Ph.D. at the Institut des Nanosciences de Paris, his research focuses on semiconductor nanocrystals, particularly in their application in electronic and optoelectronic devices.

Sandrine Ithurria is an associate professor at the Ecole Supérieure de Physiques et de Chimie Industrielles Paris PSL, in the laboratory of Physics and Materials Studies. She obtained this position in 2012 after a post-doc at the University of Chicago in the Talapin's group. Her research is dedicted to the synthesis and applications of 2D semiconductor nanoparticles from the visible to the infrared range.

James K. Utterback is a CNRS research scientist at the Institut des NanoSciences de Paris of Sorbonne Université. His research focuses on ultrafast optical spectroscopy and microscopy of energy relaxation and transport in materials for optoelectronic applications. He earned his PhD (2013-2018) as a National Science Foundation Graduate Research Fellow at the University of Colorado Boulder and then worked as a Beckman Postdoctoral Fellow at the UC Berkeley (2019-2022) before obtaining his current CNRS position in 2022.

Debora Pierucci is a CNRS researcher at Sorbonne University, France. She earned her Ph.D. from Universit Pierre et Marie Curie in 2013. Her research is centered on exploring the electronic properties of heterostructures made of low-dimensional materials, utilizing advanced photoemission techniques.

Gregory Vincent got PhD in 2008 from universite Paris XI for his work on sub wvelength mettalic grating. Since that he is working in the optics department of Onera (french aearospace lab). His activity are mostly focused on designing nanophotonics startegies for the enhancement of infrared detector performances.

Angela Vasanelli received a doctor degree in Physics from the University of Bari (Italy) in 1998 and a PhD in Solid State Physics from the University of Paris 6 in 2002. Her PhD work was a theoretical study of the electronic and optical properties of semiconductor quantum dots, realized at the Physics Department of Ecole Normale Supérieure in Paris in collaboration with the University of Lecce (Italy). In 2003 she joined as an Assistant Professor MPQ Laboratories at University Paris Diderot. She is currently Full Professor of Physics at Université Paris Cité, where she is the Director of the Denis Diderot School of Engineering. Her research activity takes place at the Physics Laboratory of the Ecole Normale Supérieure and concerns quantum optoelectronic devices, plasmonics and light-matter interaction in quantum nanostructures. She authored 80 articles published on international journals and 3 book chapters and gave 40 invited talks in international conferences. She has coordinated 4 national projects and participated to 5 national and 3 European projects.

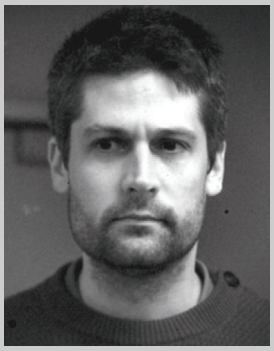

Emmanuel Lhuillier obtained engineer degree from ESPCI and a master degree in condensed matter from Univeristé Pierre and amrie Curie. He did PhD at Onera (french aeraospace lab) under supervsion of Emmanuel Rosencher working on transport properties in quantum well structure. He then joint the Guyot sionnest group as post doctoral scholar at University of Chicago, working on infrared photoconduction of colloidal nanocrystals. He then conducted a second post doc a ESPCI in Dubertret's group working on optoelectronic properties of colloidal quantum well. Since 2015, he is working as CNRS researcher on optoelectronic of confined nanomaterial in the Institut des NanoSciences de Paris from Sorbonne Université.